Article

An NMR Method for the Determination of Protein-Binding Interfaces Using Dioxygen-Induced Spin–Lattice Relaxation Enhancement

M. Sakakura, S. Noba, P. A. Luchette, I. Shimada, and R. S. Prosser

J. Am. Chem. Soc., **2005**, 127 (16), 5826-5832• DOI: 10.1021/ja047825j • Publication Date (Web): 02 April 2005

JACS
JOURNAL OF THE AMERICAN CHEMICAL SOCIETY

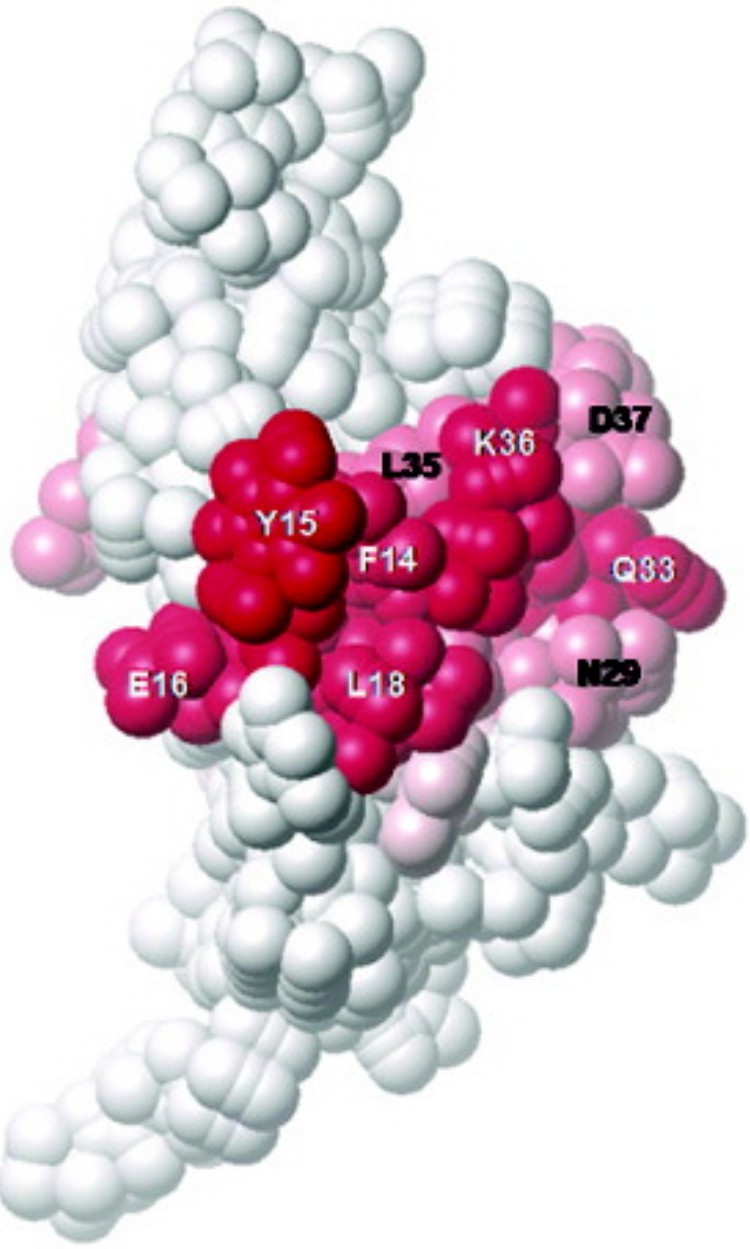

More About This Article

Additional resources and features associated with this article are available within the HTML version:

- Supporting Information

Journal of the American Chemical Society is published by the American Chemical Society. 1155 Sixteenth Street N.W., Washington, DC 20036

J|A|C|S
ARTICLES
Published on Web 04/02/2005

An NMR Method for the Determination of Protein-Binding Interfaces Using Dioxygen-Induced Spin−Lattice Relaxation Enhancement

M. Sakakura,[†] S. Noba,[†] P. A. Luchette,[‡] I. Shimada,[†,§] and R. S. Prosser*,[||]

Contribution from the Graduate School of Pharmaceutical Sciences, University of Tokyo, Hongo, Bunkyo-ku, Tokyo 113-0033, Japan, Department of Chemistry, Kent State University, P.O. Box 5190, Kent, Ohio 44242-0001, Biological Information Research Center (BIRC), National Institute of Advanced Industrial Science and Technology (AIST), Aomi, Koto-ku, Tokyo 135-0064, Japan, and Department of Chemistry, University of Toronto, UTM, 3359 Mississauga Road North, Mississauga, Ontario, Canada L5L 1C6

Received April 15, 2004; E-mail: sprosser@utm.utoronto.ca

Abstract: Using oxygen as a paramagnetic probe, researchers can routinely study topologies and protein-binding interfaces by NMR. The paramagnetic contribution to the amide ^{1}H spin−lattice relaxation rates (R_1^P) have been studied for uniformly ^{2}H,^{15}N-labeled FB protein, a 60-residue three-helix bundle, constituting the B domain of protein A. Through TROSY versions of inversion−recovery experiments, R_1^P could be determined. R_1^P was then measured in the presence of a stoichiometric equivalent of an unlabeled Fc fragment of immunoglobulin (Ig) G, and the ratio of R_1^P of the FB−Fc complex to that of free FB [i.e., R_1^P(complex)/R_1^P(free)] was determined for each observable residue. Regions of helix I and helix II, which were previously known to interact with Fc, were readily identified as belonging to the binding interface by their characteristically reduced values of R_1^P(complex)/R_1^P(free). The method of comparing oxygen-induced spin−lattice relaxation rates of free protein and protein−protein complexes, to detect binding interfaces, offers greater sensitivity than chemical shift perturbation, while it is not necessary to heavily deuterate the labeled protein, as is the case in cross saturation experiments.

Introduction

The proteomics era has brought about a need to understand protein−protein interactions and reliably identify protein-binding interfaces. In this article, we introduce an NMR approach for the determination of binding interfaces in protein−macromolecule complexes. The experiment makes use of molecular oxygen to reveal protons at the binding interface, through a comparison of the paramagnetic contribution to the ^{1}H spin−lattice relaxation rates of the free protein and the protein−protein complex. Details of our investigations on studies of the B domain of protein A (^{2}H,^{15}N-labeled FB) both free and in the presence of the Fc portion of Immunoglobulin (Ig) G will be presented and the results will be discussed in terms of current techniques for studying protein−protein interactions by NMR.

Traditionally, NMR experiments have made use of chemical shift perturbations to elucidate protein-binding interfaces.[1−3] However, chemical shift changes may originate either by a change of the chemical environment of the nuclei at the interface or by binding-induced conformational and dynamical changes.[4] Sizable chemical shift deviations commonly arise from regions in labeled proteins not associated with a binding site.[1] Experiments that measure properties associated with hydrogen exchange dynamics[5] or backbone and side chain dynamics are also often sensitive to protein binding. Such measurements range from simple observations of differential line-broadening to more sophisticated studies of dynamics through (indirectly detected) ^{2}H relaxation rates.[6] A broad variety of experiments utilize nuclear Overhauser effects (NOEs) to sleuth out intermolecular proton−proton contacts.[7] Since the magnitude of the NOE has a $1/r^6$ dependence on interproton distances, such contacts are frequently within 5 Å, and isotope editing strategies can be combined to filter NOEs, for example, from unlabeled protein to labeled protein.[8] NOE-based strategies for identifying protein-binding interfaces work well under conditions of strong binding.[9−11] Cross saturation is governed by the same relaxation mechanism but makes use of excitation confined to the unlabeled

[†] University of Tokyo.
[‡] Kent State University.
[§] AIST.
[||] University of Toronto.

(1) Chen, Y.; Reizer, J.; Saier, M. H.; Fairbrother, W. J.; Wright, P. E. *Biochemistry* **1993**, *32*, 32−37.
(2) Gronenborn, A. M.; Clore, G. M. *J. Mol. Biol.* **1993**, *233*, 331−335.
(3) Shuker, S. B.; Hajduk, P. J.; Meadows, R. P.; Fesik, S. W. *Science* **1996**, *274*, 1531−1534.
(4) Foster, M. P.; Wuttke, D. S.; Clemens, K. R.; Jahnke, W.; Radhakrishnan, I.; Tennant, L.; Reymond, M.; Chung, J.; Wright, P. E. *J. Biomol. NMR* **1998**, *12*, 51−71.
(5) Englander, S. W.; Mayne, L.; Bai, Y.; Sosnick, T. R. *Protein Sci.* **1997**, *6*, 1101−1109.
(6) Kay, L. E.; Muhandiram, D. R.; Farrow, N. A.; Aubin, Y.; Forman-Kay, J. D. *Biochemistry* **1996**, *35*, 361−368.
(7) Otting, G.; Wuthrich, K. *J. Am. Chem. Soc.* **1989**, *111*, 1871−1875.
(8) Fesik, S. W.; Luly, J. R.; Erickson, J. W.; Abadzapatero, C. *Biochemistry* **1998**, *27*, 8297−8301.
(9) Spronk, C. A. E. M.; Bonvin, A. M. J. J.; Radha, P. K.; Melacini, G.; Boelens, R.; Kaptein, R. *Struct. Folding Des.* **1999**, *7*, 1483−1492.
(10) Garrett, D. S.; Seok, Y. J.; Peterkofsky, A.; Gronenborn, A. M.; Clore, G. M. *Nat. Struct. Biol.* **1999**, *6*, 166−173.
(11) Varani, L.; Gunderson, S. I.; Mattaj, I. W.; Kay, L. E.; Neuhaus, D.; Varani, G. *Nat. Struct. Biol.* **2000**, *7*, 329−335.

10.1021/ja047825j CCC: $30.25

target molecule and subsequent detection of signal intensity of the (^{15}N-) labeled protein.[12] Transfer of magnetization from the target to the labeled protein is based on spin-diffusion, and mixing times are therefore sufficiently long that the experiment can be used to detect interfaces with unsurpassed sensitivity for both strong and weak protein complexes.[13] To selectively excite the target molecule and to avoid spurious cross saturation effects to protons not associated with the binding interfaces, the labeled protein must be fully deuterated while the solvent ^2H_2O fraction is typically 80−95%. Consequently, detection of intermolecular interactions through cross saturation experiments is challenging from the perspective of signal-to-noise.

Theory and Background

Paramagnetic species are also used to map binding interfaces in proteins. A strongly relaxing species, such as gadolinium, complexed to a small chelate, is commonly added to relax solvent-exposed resonances.[14−16] Alternatively, a water soluble organic free radical such as a nitroxyl (TEMPO) derivative may be used.[16,17] The electronic relaxation time of these species is on the order of nanoseconds, and strong spin−lattice relaxation enhancement and line-broadening is observed for most resonances associated with the protein surface. Upon addition of a target macromolecule, nuclei at the binding interface are protected from the relaxation agents. A comparison of line-broadening in spectra of the labeled protein, with and without the binding partner, will thus reveal the interface. Limitations to this approach include the fact that the water soluble paramagnetic agents typically exhibit a strong preference for certain residues. For example, diethylene triaminepentaacetic acid (DTPA) moieties, chelated to gadolinium, preferentially associate with charged complexes on the surface of proteins and may also interact with surface residues whose oxygen atoms act as coordinating nucleophiles to lanthanides.[16] Conversely, TEMPO derivatives preferentially associate with hydrophobic residues,[16] though derivatives of TEMPO are less biased.[18] Because of the size of these paramagnetic complexes and organic radicals, local surface mobility also plays a role in determining the magnitude of the paramagnetic effect, and the correlation between surface accessibility and paramagnetic effect may be difficult to establish. Paramagnetic spin labels may also be positioned on or near the binding site of the unlabeled protein by first replacing a specific nonconserved residue with cysteine. Nitroxide spin labels may then be covalently attached to the free cysteine moiety. Clearly, ^{1}H resonances associated with residues from the labeled protein will be selectively broadened at or near the binding site, in a $1/r^6$ distance-dependent fashion.[19]

Recently, several NMR articles have described the use of oxygen as a paramagnetic probe of protein topology in the case of both water soluble proteins[20−23] and membrane proteins.[24] Oxygen has several advantages in NMR studies of topology. First, the collisional cross section of oxygen is sufficiently small that it can accurately sample convoluted protein surfaces. Equally important, studies thus far indicate no significant propensity of O_2 to interact with a specific residue or chemical group,[20,21] although Teng et al. have observed weak associative interactions between oxygen and hydrophobic protein crevices or surfaces, particularly in regions undergoing greater fluctuations.[25] Oxygen can be easily incorporated by application of a desired partial pressure, for a sufficient period of time. Moreover, as discussed below, oxygen electronic relaxation times are sufficiently short to simplify the analysis of paramagnetic effects. A second consequence of the short electronic relaxation time is that line-broadening is relatively weak at partial pressures where significant paramagnetic spin−lattice relaxation rates and chemical shift perturbations are observed (i.e., 10−30 atm). The paramagnetic spin−lattice relaxation rate, R_1^P, is obtained by measuring T_1 at a desired oxygen partial pressure and the equivalent partial pressure for nitrogen. Then,

$$R_1^{\,P} = 1/T_1(O_2) - 1/T_1(N_2) \qquad (1)$$

In the extreme narrowing regime, the paramagnetic contribution to spin−lattice relaxation, $1/T_1^P$, is equal to that for transverse relaxation, $1/T_2^P$, although T_1 effects are simply easier to measure since ambient spin−lattice relaxation times are so much longer than transverse relaxation rates for macromolecules. To the extent that paramagnetic spin−lattice relaxation is acted on purely by a dipolar interaction between a nuclear spin, I, and a paramagnetic spin, S, the relaxation rate may be described by the classic equation[26,27]

$$R_1^{\,P} = \frac{2}{15}\gamma_I^{\,2}\gamma_S^{\,2}\hbar^2 S(S+1)[J_0(\omega_I - \omega_S) + 3J_1(\omega_I) + 6J_2(\omega_I + \omega_S)] \qquad (2)$$

For a freely diffusing paramagnet such as oxygen, the dipolar interaction is modulated principally by translational diffusion and by fast electronic spin relaxation. Consequently, the classic Solomon, Bloembergen, Morgan equations[28,29] do not apply, nor are the above spectral density functions necessarily Lorentzian. The problem of a freely diffusing paramagnet, with electronic relaxation times, T_1^S and T_2^S, has been treated by Hwang and Freed, wherein the spectral density function is described by[30]

$$J_k(\omega) = \frac{8}{27}\frac{N_A[O_2]}{bD} \times \mathrm{Re}\left\{\left[1 + \frac{1}{4}(i\omega\tau + \tau/T_k^{\,S})^{1/2}\right]/\left[1 + (i\omega\tau + \tau/T_k^{\,S})^{1/2} + \frac{4}{9}(i\omega\tau + \tau/T_k^{\,S})^{1/2} + \frac{1}{9}(i\omega\tau + \tau/T_k^{\,S})^{3/2}\right]\right\} \qquad k = 1,2 \qquad (3)$$

where b represents the distance of closest approach for the oxygen species to the nucleus of interest and D signifies the

(12) Takahashi, H.; Nakanishi, T.; Kami, K.; Arata, Y.; Shimada, I. *Nat. Struct. Biol.* **2000**, *7*, 220−223.
(13) Nakanishi, T.; Miyazawa, M.; Sakakura, M.; Terasawa, H.; Takahashi, H.; Shimada, I. *J. Mol. Biol.* **2002**, *318*, 245−249.
(14) Kopple, K. D.; Schamper, T. J. *J. Am. Chem. Soc.* **1972**, *94*, 3644−3646.
(15) Niccolai, N.; Valensin, G.; Rossi, C.; Gibbons, W. A. *J. Am. Chem. Soc.* **1982**, *104*, 1534−1537.
(16) Petros, A. M.; Mueller, L.; Kopple, K. D. *Biochemistry* **1990**, *29*, 10041−10048.
(17) Esposito, G.; Lesk, A. M.; Molinari, H.; Motta, A.; Niccolai, N.; Pastore, A. *J. Mol. Biol.* **1992**, *224*, 659−670.
(18) Niccolai, N.; Spiga, O.; Bernini, A.; Scarselli, M.; Ciutti, A.; Fiaschi, I.; Chiellini, S.; Molinari, H.; Temussi, P. A. *J. Mol. Biol.* **2003**, *332*, 437−447.
(19) Scherf, T.; Hiller, R.; Anglister, J. *FASEB J.* **1995**, *9*, 120−126.
(20) Teng, C. L.; Bryant, R. G. *J. Am. Chem. Soc.* **2000**, *122*, 2667−2668.
(21) Hernandez, G.; Teng, C. L.; Bryant, R. G.; LeMaster, D. M. *J. Am. Chem. Soc.* **2002**, *124*, 4463−4472.
(22) Ulmer, T. S.; Campbell, I. D.; Boyd, J. *J. Magn. Reson.* **2002**, *157*, 181−189.
(23) Ulmer, T. S.; Campbell, I. D.; Boyd, J. *J. Magn. Reson.* **2004**, *166*, 190−201.
(24) Luchette, P. A.; Prosser, R. S.; Sanders, C. R. *J. Am. Chem. Soc.* **2002**, *124*, 1778−1781.
(25) Teng, C.; Bryant, R. G. *Biophys. J.* **2004**, *86*, 1713−1725.

sum of the diffusion constants of both species. Finally, τ is defined by $\tau = b^2/D$. For the spectral density terms at the ^{1}H Larmor frequency (i.e., a Larmor frequency of 600 MHz in our study) the limiting case of $\omega T_k^S \ll 1$ should apply since $T_k^S \approx 7.5 \times 10^{-12}$ s.[31] Moreover, we may approximate $\tau/T_k^S \gg 1$, assuming $D = 2 \times 10^{-9}$ m^2 s^{-1} and $b \geq 2.6 \times 10^{-10}$ m, in which case Hwang and Freed have shown that the expression for the spectral density function simplifies in the extreme narrowing limit to

$$J_k(\omega) \approx J(0) = \frac{2}{3}\frac{N_A[O_2]}{b^3}T_k^S \qquad (4)$$

The above approximations are the result of a force-free approach (i.e., the O_2 probability distribution function is a constant as long as the dipole distance, r, is equal to or greater than b). Recently, Teng and Bryant have extended the above theory by introducing a geometric parameter that includes both a steric term accounting for relative oxygen accessibility and a soft potential term accounting for changes in local concentrations of the paramagnet, near the nucleus of interest.[32] The problem of accurately simulating dioxygen-induced paramagnetic rates is no doubt compounded by variations in the oxygen solubility and diffusion rate, diffusional jump length, and water binding. Certainly, our simulations of paramagnetic rates from oxygen acting on a protein surface go beyond the intentions of the original Freed articles. However, this article focuses on the use of oxygen in elucidating the binding interface, and we are therefore more concerned with changes in the R_1^P profile upon binding.

Herein, we present results of measurements of R_1^P of amide protons from ^{2}H,^{15}N-labeled FB both free and in the presence of the binding protein, Fc. Thus, in all there are four critical experiments: ^{1}H spin−lattice relaxation measurements of the free protein and of the complex at 20 atm P_{O2} and equivalent experiments under nitrogen. We will begin with a brief discussion of the simulations, followed by an analysis of R_1^P of FB in both the free and Fc-bound state, after which the method will be discussed in light of other NMR methods to detect interfaces of bound proteins.

Methods

Sample Preparation. Uniformly ^{2}H,^{15}N-labeled FB was prepared by growing *Escherichia coli* in M9 media, in ^2H_2O, using $^{15}NH_4Cl$, ^{2}H-glucose, and ^{2}H,^{15}N-Celtone (Spectra Stable Isotopes, Columbia, MD) as the sole nitrogen and deuterium source. ^{2}H,^{15}N-labeled FB was isolated and purified as described.[33] The 460-residue humanized murine IgG (RNOK203) was prepared as described.[34] The Fc fragment of RNOK203 was obtained by enzymatic digestion with metalloendopeptidase as described.[35]

NMR Experiments. Samples consisted of 1 mM ^{2}H,^{15}N-labeled FB, free or in the presence of stoichiometric equivalents of the unlabeled Fc. Oxygen partial pressures (20 atm) were applied to the samples for a period of 2−3 days, in a water bath equilibrated to the experimental temperature (298 K), before use in the spectrometer. This allowed for full equilibration of oxygen in the solution, as judged by monitoring ^{1}H spin−lattice relaxation times of the buffer. Control experiments were also performed using N_2 as a pressure source at 20 atm. Sapphire NMR sample tubes were obtained from Saphikon (Milford, NH). These 5-mm NMR tubes have a 1-mm wall thickness. The NMR tubes were epoxied to a 1/8 in. Swagelok stainless steel gas line. To ensure a constant pressure during the experiment, the gas line was fully open to the regulator and tank.

There are several hazards associated with the use of oxygen in NMR studies. Over prolonged periods, proteins (in particular, cysteine residues) may become oxidized. Though we did not observe any deleterious effects over a time span of 1 month, one useful precaution is to incorporate 50 mM dithiothreitol (DTT) in protein samples. Second, levitation effects are observed above 30 atm oxygen partial pressures at field strengths of 600 MHz (^{1}H). This effect can be alleviated by implementing a gas-permeable frit above the meniscus of the sample in the NMR tube, assuming high pressures are desired. For safety, pressures in excess of 15 atm should probably not be attempted without sapphire tubes.

NMR experiments were carried out at 298 K, on a Bruker Avance 600 MHz instrument. Spin−lattice relaxation rates were measured via an inversion recovery period (i.e., $180_x - \tau$), followed by a ^{1}H−^{15}N TROSY sequence.[36] The 180_x inversion pulse was usually replaced with consecutive 90_x90_{-x} pulses in alternate scans, so that the net signal observed in the 2D spectrum, with appropriate phase cycling, decayed to zero with increasing recovery periods, τ. 2D spectra were acquired using eight scans per increment for free FB and 16 scans per increment for the FB−Fc complex. All 2D spectra were acquired using 128 increments in the ^{15}N dimension. Repetition times were set to 3−5 s in the presence of oxygen and 6−12 s in the presence of nitrogen. Processing was performed using Xwinnmr; signal intensities were obtained from the series of 2D spectra and fitted to single-exponential decay curves. In the case of the inversion recovery experiments, τ for free FB ranged from 0.001 to 8 s under nitrogen and 0.001 to 1.5 s in the presence of oxygen. In contrast, the maximum τ-values used for the FB−Fc complex were 1.2 s under nitrogen and 0.2 s under oxygen. In principle, spin−lattice relaxation in highy deuterated proteins may turn out to be poorly approximated as a single-exponential process. However, the overall spin−lattice relaxation rates at 20 atm are dominated by the paramagnetic contribution so that even 20% errors in the spin−lattice relaxation rates under nitrogen have a negligible effect. In studies of FB and the FB−Fc complex, a TROSY sequence was used to detect amide proton signal after an inversion recovery sequence as discussed above. Longitudinal two-spin order (I_ZN_Z) was also measured via an I_ZN_Z TROSY experiment (data not shown).[37,38] Profiles for paramagnetic spin−lattice relaxation rates associated with I_ZN_Z were similar to those obtained from an inversion recovery spin−lattice relaxation experiment.

Simulations of Paramagnetic Spin−Lattice Relaxation Rates. The distance of closest approach, b, and $1/b^3$ were estimated for each amide proton from a high resolution structure by simply considering a spherical volume of radius 10 Å centered about each amide proton and consisting of grid points spaced 0.05 Å apart along three orthogonal axes in a

(26) Hwang, L.; Freed, J. H. *J. Chem. Phys.* **1975**, *63*, 4017−4025.
(27) Ayant, Y.; Belorizky, E.; Alizon, J.; Gallice, J. *J. Phys. I* **1975**, *36*, 991−1004.
(28) Solomon, I.; Bloembergen, N. *J. Chem. Phys.* **1956**, *25*, 261−266.
(29) Bertini, I.; Luchinat, C. *NMR of Paramagnmetic Molecules in Biological Systems*; Benjamin/Cummings: Menlo Park, CA, 1986.
(30) Freed, J. H. *J. Chem. Phys.* **1978**, *68*, 4034−4037.
(31) Teng, C. L.; Hong, H.; Kiihne, S.; Bryant, R. G. *J. Magn. Reson.* **2001**, *148*, 31−34.
(32) Teng, C.; Bryant, R. G. *Biophys. J.*, submitted for publication, 2005.
(33) Torigoe, H.; Shimada, I.; Saito, A.; Sato, M.; Arata, Y. *Biochemistry* **1990**, *29*, 8787−8793.
(34) Nishihara, T.; Ushio, Y.; Higuchi, H.; Kayagaki, N.; Yamaguchi, N.; Soejima, K.; Matsuo, S.; Maeda, H.; Eda, Y.; Okumura, K.; Yagita, H. *J. Immunol.* **2001**, *167*, 3266−3275.
(35) Yamaguchi, Y.; Kim, H.; Kato, K.; Masuda, K.; Shimada, I.; Arata, Y. *J. Immunol. Methods* **1995**, *181*, 259−267.
(36) Pervushin, K.; Riek, R.; Wider, G.; Wuthrich, K. *Proc. Natl. Acad. Sci. U.S.A.* **1997**, *94*, 12366−12371.
(37) Damberg, P.; Jarvet, J.; Allard, P.; Graslund, A. *J. Biomol. NMR* **1999**, *15*, 27−37.
(38) Wang, C.; Palmer, A. G., III. *Magn. Reson. Chem.* **2003**, *41*, 866−876.

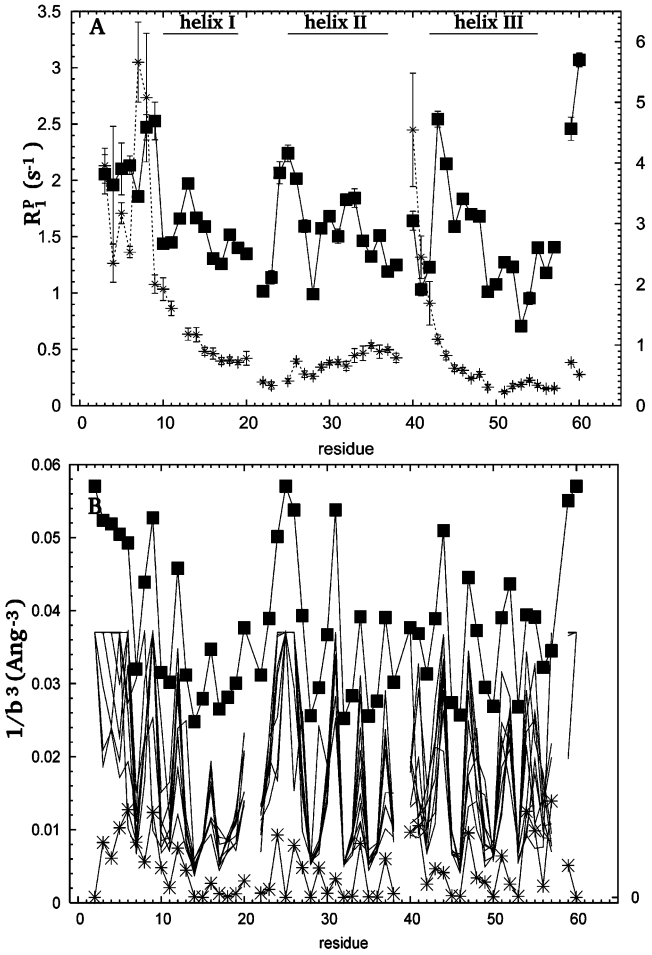

Figure 1. (A) Experimental profile of paramagnetic spin−lattice relaxation rates, R_1^P (designated by ■), as a function of residue for the free protein, FB. Paramagnetic spin−lattice relaxation rates were determined by measuring the difference between the $1/T_1$ in an inversion recovery experiment at 20 atm partial pressure of oxygen. R_1^P was then determined by measuring inversion recovery rates under nitrogen at 20 atm (designated by *) and calculating the difference between the spin−lattice relaxation rates from the two environments. (B) Theoretical evaluation of $1/b^3$, determined for each of nine NMR-derived ensemble structures of free FB protein. The solid black line connecting the ■'s represents the average of the $1/b^3$ profiles, vertically displaced for clarity. The rms deviation from the average profile is given by dashed line (*).

molecule fixed coordinate system.[20,21] A computer program was used that evaluates each grid point and first determines if a protein atom occupies the point within its van der Waals radius. If the grid point is free, the program next determines if an oxygen molecule can fit on the grid point, that is, if the distance to the nearest protein atom, minus its van der Waals radius, is more than the radius of an oxygen molecule. Here we use an effective oxygen radius of 1.5 Å.[39] Assuming the oxygen molecule does not overlap with other atoms on the grid point, the distance of closest approach, b, and hence, $1/b^3$, are determined. In principle, one would need to be concerned with enclosed free volumes in proteins. However, the FB protein is too small to be concerned with this complication. To account for the dynamical variation of conformations and, thus, local oxygen accessiblities to amide groups, nine separate PDB files of the FB protein, derived from a previous NMR structure study of free FB, were used to predict an average $1/b^3$ profile as shown in Figure 1B. This procedure was facilitated by the use of a cluster server, with independent processors so that each ensemble structure could be evaluated simultaneously. The profile was then fitted, using a single proportionality constant, to the observed paramagnetic spin−lattice relaxation rates. The procedure for simulating $1/b^3$ for the FB amide protons in the FB−Fc complex is similar except that the PDB file is obtained from an X-ray structure study, and no ensemble of structures is considered. In both cases, protons were added to the protein structures using MOLMOL viewing and structure manipulation software.[40]

Results and Discussion

Figure 1A compares the paramagnetic spin−lattice relaxation rate profile of free FB protein at 20 atm oxygen partial pressure, obtained from an inversion recovery experiment. In contrast, the proton spin−lattice relaxation rates of FB, under 20 atm N_2, bear no resemblance to the paramagnetic rate profile. Figure 1B displays the theoretical $1/b^3$ profile for the amide protons, predicted for each of the nine lowest energy NMR-derived ensemble structures. Note that, in regions where the backbone structure is not well-defined, $1/b^3$ varies considerably between each model, as shown by the rms deviations of $1/b^3$ also displayed in Figure 1B. In the extreme narrowing limit and assuming that the spin−lattice relaxation term associated with dynamics plays a minor role, $1/b^3$ should be directly proportional to the observed paramagnetic spin−lattice relaxation rates. There is a good qualitative correspondence between the observed paramagnetic rates (Figure 1A) and profile predicted by the average of $1/b^3$ for the nine ensemble structures. Note that, for example, a local maximum paramagnetic rate is observed for the amide proton of Glu 25, which is also the most exposed to solvent and thus to oxygen, as predicted by the $1/b^3$ calculation. However, the relative heights of local maxima are not well-reproduced by the simulation. Residual dipolar couplings and additional NOE experiments are ongoing in an effort to refine the NMR-derived structure of FB.[41] Local bias due to geometric factors (i.e., relative accessible surface area of residues) or due to preferential interactions between oxygen and certain residues may also contribute to the difficulty in reproducing the paramagnetic rate profile quantitatively from a $1/b^3$ calculation alone.[32]

Proton chemical shifts are nearly invariant with oxygen pressure over the range investigated, which is also consistent with the notion that oxygen does not exhibit binding to any residues. As with previous studies of proteins at low pressures, the absence of ^{1}H chemical shift perturbations also clearly shows that there are no pressure-induced conformational changes of FB at or below 20 atm. This is not surprising since protein compressibilities are such that pressures less than 100 atm rarely affect enzyme structure or activity.[42,43]

The addition of stoichiometric equivalents of the Fc protein domain, from IgG, results in a relatively tight complex between Fc and FB. As shown in Figure 2A, chemical shift perturbations, induced by the binding of FB to Fc, are significant, particularly near the N-terminus. However, there is no clear pattern of shift perturbations associated with helices I and II, which are known to form the FB−Fc-binding interface.[12,13,44] Moreover, the shift perturbations induced by a change of environment through formation of the complex cannot be distinguished from binding-

(39) Marrink, S. J.; Berendsen, H. J. C. *J. Phys. Chem*. **1996**, *100*, 16729−16738.
(40) Konradi, R.; Billeter, M.; Wüthrich, K. *J. Mol. Graphics* **1996**, *14*, 51−55.
(41) Shimada, I. University of Tokyo and AIST. Personal communication.
(42) Heremans, K. *Biochim. Biophys. Acta Protein Struct. Mol. Enz.* **1998**, *1386*, 353−370.
(43) Taulier, N.; Chalikian, T. V. *Biochim. Biophys. Acta Protein Struct. Mol. Enz*. **2002**, *1595*, 48−70.
(44) Deisenhofer, J. *Biochemistry* **1981**, *20*, 2361−2370.

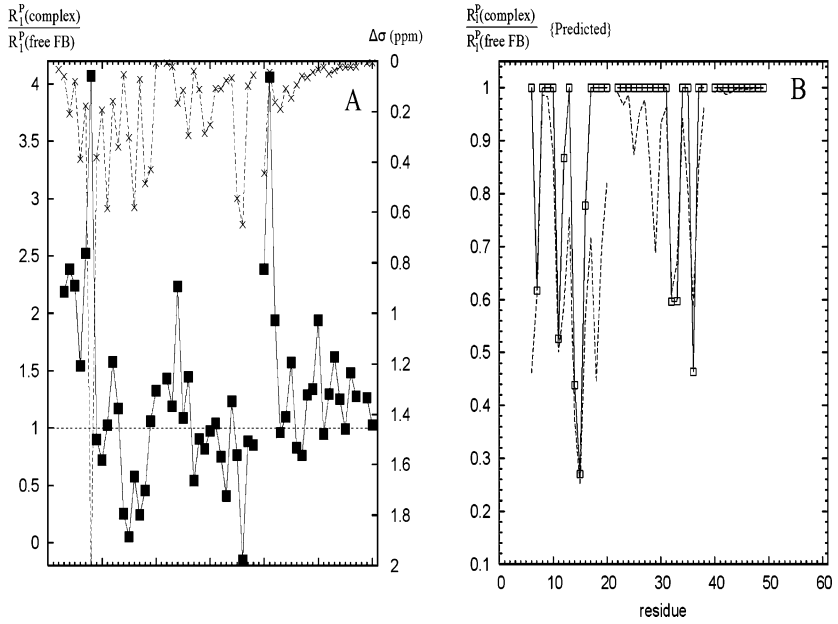

Figure 2. (A) Experimental measurements of the ratio of paramagnetic spin−lattice relaxation rates of FB when complexed with Fc to those of FB in the absence of binding protein [i.e., R_1^P(complex)/R_1^P(free), represented by black ■]. Chemical shift perturbations induced by the binding of FB to Fc are represented by crosses. Shift perturbations are calculated from the magnitude of changes of both ^{1}H and ^{15}N shifts, according to $\sqrt{0.5\times\{[\Delta\sigma(^1\mathrm{H})]^2+[0.25\times\Delta\sigma(^{15}\mathrm{N})]^2\}}$. (B) Simulation of R_1^P(complex)/R_1^P(free), based on a calculation of $1/b^3$ (—) of FB backbone amide protons for the protein complex and free FB. This same ratio was also calculated on the basis of the volume integral $\int dV/r^6$ (− − −), where r represents all possible oxygen to nuclear spin distances and only volume elements outside the van der Waals radii of oxygen and all protein atoms were considered. The X-ray crystal structure of FB−Fc was used to estimate $1/b^3$, while the Fc domain was removed and the calculations were repeated to estimate R_1^P(free). Thus, this calculation assumes no conformational changes induced by binding. Note that residues 51−60 are not defined in the crystal structure of the complex; hence, R_1^P(complex)/R_1^P(free) cannot be predicted for this region. Studies by Gouda et al. suggest that prominent binding-induced conformational changes of FB arise in part from crystal contacts.[46]

induced conformational changes. If oxygen were to serve as a useful paramagnetic probe of binding interfaces, we would expect to see significantly reduced spin−lattice relaxation rate enhancement at the interface, assuming the complex is reasonably strong. To factor out topological effects, we can compare the ratio of paramagnetic spin−lattice relaxation rates of FB when complexed with Fc to those of FB in the absence of binding protein [i.e., R_1^P(complex)/R_1^P(free)]. If this ratio is less than 1.0 we can conclude that some degree of protection from oxygen accessibility is offered by formation of the FB−Fc complex. In examining the experimentally determined R_1^P-(complex)/R_1^P(free) profile, shown in Figure 2A, it is clear that there are two regions, corresponding to the latter two turns of both helix I and helix II, which exhibit a pronounced decrease in oxygen accessibility upon binding. There are also many key residues, not associated with the binding interface, for which R_1^P(complex)/R_1^P(free) is considerably greater than 1. For example, the paramagnetic spin−lattice relaxation rates associated with Lys 8, Ser 40, and Gln 41 all increase upon formation of the complex. We attribute these changes to binding-induced conformational changes, which is also reinforced by observable chemical shift changes in each case. The amide paramagnetic rate for Asn 24 is also curiously high, particularly in light of the fact that there is no chemical shift perturbation associated with this residue. However, the resonance for Asn 24 overlaps with Asn 4, giving rise to an averaging of paramagnetic rates for the observed peak. Last, we observe a pronounced oscillation in R_1^P(complex)/R_1^P(free) for residues originating from helix III, which is known not to be involved in the FB−Fc complex. Moreover, the amplitude of these oscillations decreases toward the carboxyl terminus of the protein, as do the chemical shift perturbations. The local maxima are associated with the inner face of helix III (i.e., residues 50, 53, and 56), which coincidentally have the lowest paramagnetic rates for free FB, since the helix is in direct contact with the FB protein interior. Therefore, we speculate that upon binding, helix III tilts away from the FB interior, creating the greatest change in oxygen exposure to the face of helix III, which was formally buried in the free FB conformation. Clearly, conformational changes have a significant impact on the paramagnetic rates. However, the striking decrease in R_1^P(complex)/R_1^P(free) for helices I and II still allows us to unambiguously define the binding interface.

Figure 2B represents a simulation of R_1^P(complex)/R_1^P(free), based on a calculation of $1/b^3$ of FB backbone amide protons for the protein complex and for free FB, as shown by the solid line. In both cases, the X-ray crystal structure of the FB−Fc complex[44] was used to estimate $1/b^3$. Thus, the paramagnetic rates for free FB were estimated simply by removing all atoms belonging to Fc. This approach allows us to examine the potential changes in paramagnetic rates, R_1^P, associated with elucidating the binding interface, without simultaneously considering the complication of binding-induced conformational changes. The result predicts a strong effect of binding on R_1^P-(complex)/R_1^P(free) for both helices I and II. R_1^P(complex)/R_1^P-(free) was also simulated, as shown by the dashed line, by separately evaluating the volume integral, $\int dV/r^6$, for both the complex and the free FB protein. The variable r represents all possible oxygen−nuclear distances for each amide proton of interest. The numerical integral calculation, which followed the same approach taken by others,[21] excluded all possible volume elements where r was less than the sum of the van der Waals radius of oxygen plus that of the respective protein atoms. Note

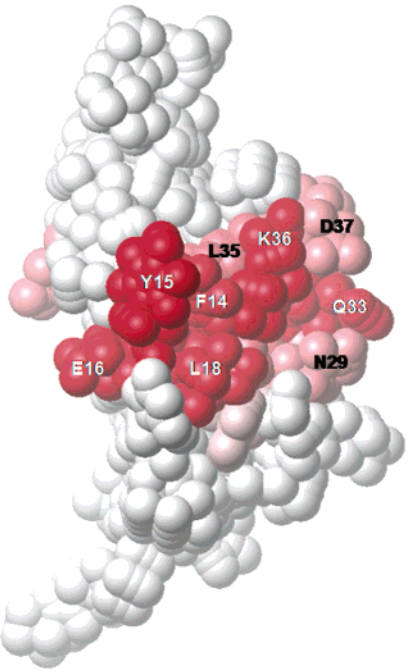

Figure 3. Depiction of R_1^P(complex)/R_1^P(free) mapped onto FB. A gradation of red (strongest binding or greatest change of O_2 accessibility upon binding) to white (no binding) is assigned to residues depending on the magnitude of R_1^P(complex)/R_1^P(free).

that if there were no other protein atoms obstructing oxygen from an amide proton, the volume integral would give $1/b^3$. Thus, $\int dV/r^6$ in one sense accounts for geometrical factors or biases associated with accessible surface areas for given residues. The result of this calculation reveals that one side of turns 2 and 3 of both helices I and II is predicted to strongly interact with Fc, while turn 1 is also in contact with Fc. The experimental observation, shown in Figure 2A, essentially reflects this observation except that there does not appear to be any protection associated with turn 1 of either helix I or helix II. However, the chemical shift perturbation profile, also shown in Figure 2A, clearly reveals dramatic shifts upon binding for the first turn of helices I and II, suggesting that the paramagnetic rate of FB in this region is not reduced, upon binding to Fc, due to conformational changes.

Figure 3 represents the NMR-derived structure of FB where values of R_1^P(complex)/R_1^P(free) less than 1 have been mapped onto the protein surface. Those residues whose experimentally determined ratio, R_1^P(complex)/R_1^P(free), is closest to 0 are denoted as deep red, while any residues for which this value is greater than 1 are left as white. A clear binding interface is revealed that is consistent with former studies of the binding interface based on the X-ray crystal structure of the complex[44] or cross saturation experiments by Shimada and co-workers.[12,13]

Concluding Remarks

Although chemical shift perturbations are routinely used to determine binding interfaces, they suffer from sensitivity to local conformational changes. Paramagnetic spin−lattice relaxation rates are also sensitive to conformational or topological changes, although the ratio, R_1^P(complex)/R_1^P(free), appears to be more robust in terms of identifying binding regions. Taken together, chemical shift perturbations and oxygen-induced protection factors give a good indication of the binding interface. Furthermore, although this study focused on protein−protein interactions by monitoring the backbone (amide) signal, it is anticipated that side chain paramagnetic rates would be at least as sensitive to the effects of binding. In comparing our results to one of the most definitive methods for the study of protein−protein interactions, namely, cross saturation experiments, our conclusions were similar, and it is useful to contrast the two techniques. The determination of binding interfaces using oxygen-induced spin−lattice relaxation enhancement does not rely on extensive deuteration of either the protein or the solvent, though protein deuteration is a necessary evil in TROSY studies of very large complexes. Indeed, since oxygen significantly decreases both solvent and protein ^{1}H spin−lattice relaxation times, spin-diffusion effects are diminished and local spin−lattice relaxation times are more meaningful. While cross saturation experiments require $H_2O/^2H_2O$ ratios between 0.05 and 0.10, studies of binding interfaces using oxygen can easily tolerate 90% H_2O. Thus, R_1^P(complex)/R_1^P(free) measurements are comparatively sensitive. On the other hand, the analysis of oxygen-induced spin−lattice relaxation enhancement reveals that binding-induced conformational changes can complicate matters, though not as fatally as in the case where chemical shift perturbations are used alone. Therefore, cross saturation effects seem to be the most independent of conformational changes and remain the most conclusive for binding studies by NMR, though studies that use paramagnetic spin−lattice relaxation rates in the presence of oxygen require less experimental time. Finally, this study focused on a protein complex with a relatively low dissociation constant. In cases where binding is not tight, the use of oxygen-induced paramagnetic spin−lattice relaxation rates should be effective so long as the bound state is prevalent, since the paramagnetic rate will be a weighted average of the bound and free states. In contrast, the method of cross saturation is applicable to strong and weak protein complexes.[45]

In summary, the use of oxygen to resolve binding interfaces by NMR offers clear advantages over the use of chemical shift perturbations, while the experiments offer high sensitivity with minimal effort needed in deuteration or labeling. In comparison to the use of other paramagnetic probes such as organic free radicals or lanthanide complexes, oxygen can be easily added and removed, with no particular preference for a given residue. Last, it is anticipated that these experiments could easily be extended to side chains, and either binding partner can be studied. It is also likely, at least in studies involving hydrophobic binding pockets, that oxygen should serve as an effective "amplifier" or contrast agent for screening binding ligands in a manner similar to the relaxation enhancement approach discussed in this article (i.e., SAR by NMR using paramagnetic spin−lattice relaxation rate enhancements of appropriately labeled proteins).

Acknowledgment. R.S.P. gratefully acknowledges the American Chemical Society (PRF AC Grant 376620) and the Natural Sciences and Engineering Research Council of Canada (NSERC) for generous funding support. R.S.P. also gratefully acknowledges the Japan Society for the Promotion of Science (JSPS) for direct funding of this research and the opportunity to interact

(45) Nakanishi, T.; Miyazawa, M.; Sakakura, M.; Terasawa, H.; Takahashi, H.; Shimada, I. *J. Mol. Biol.* **2002**, *318*, 245−249.
(46) Gouda, H.; Torigoe, H.; Saito, A.; Sato, M.; Arata, Y.; Shimada, I. *Biochemistry* **1992**, *31*, 9665−9672.

with the Japanese scientific community. This work was supported by a grant from the Japan New Energy and Industrial Technology Development Organization (NEDO). We thank Dr. Ko Okumura and Dr. Hiroaki Maeda for preparation of the IgG used in these studies. We are also grateful to Dr. Hideo Takahashi for assistance implementing pulse sequences. We thank Prof. R. G. Bryant for very helpful criticisms.

JA047825J